Steel and Composite Structures, *Vol. 21, No. 5 (2016) 1085-1103*
DOI: http://dx.doi.org/10.12989/scs.2016.21.5.1085

Elastic properties of CNT- and graphene-reinforced nanocomposites using RVE

Dinesh Kumar* and Ashish Srivastava [a]

Mechanical Engineering Department, *Malaviya National Institute of Technology*, *Jaipur 302017*, *India*

(*Received May 25, 2015, Revised June 17, 2016, Accepted July 25, 2016*)

Abstract. The present paper is aimed to evaluate and compare the effective elastic properties of CNT- and graphene-based nanocomposites using 3-D nanoscale representative volume element (RVE) based on continuum mechanics using finite element method (FEM). Different periodic displacement boundary conditions are applied to the FEM model of the RVE to evaluate various elastic constants. The effects of the matrix material, the volume fraction and the length of reinforcements on the elastic properties are also studied. Results predicted are validated with the analytical and/or semiempirical results and the available results in the literature. Although all elastic stiffness properties of CNT- and graphene-based nanocomposites are found to be improved compared to the matrix material, but out-of-plane and in-plane stiffness properties are better improved in CNT- and graphene-based nanocomposites, respectively. It is also concluded that long nanofillers (graphene as well as CNT) are more effective in increasing the normal elastic moduli of the resulting nanocomposites as compared to the short length, but the values of shear moduli, except G_{23} of CNT nanocomposite, of nanocomposites are slightly improved in the case of short length nanofillers (i.e., CNT and graphene).

Keywords: carbon nanotubes (CNT); graphene; representative volume element (RVE), nanocomposites; homogenization; elastic properties

1. Introduction

Discovery of carbon nanotubes (CNTs) (Iijima 1991) attracted the attention of researchers and scientists from all over the world in nanoscience of materials to explore and unlock the potential at the nanoscale in various technological fields. CNTs, an allotrope of carbon constituting of long-chained molecules of carbon with carbon atoms arranged in a hexagonal network to form a tubular structure, has displayed the combination of superlative mechanical, thermal and electronic properties, not possessed by any of the previous materials. There has been great interest in the last two decades in nanocomposites based on nanotubes, nanoparticles or nanosheets. Because of exceptionally novel and unique properties of CNTs, such as low weight, high stiffness, strength and resilience, CNTs are ultimate reinforcing agent, called nanofibers, in different matrix materials for the development of a new class of nanocomposites that are extremely strong and ultra-light (Ruoff *et al*. 2003, Sears and Batra 2004, Coleman *et al*. 2006, Laurent *et al*. 2010). Qian *et al*.

*Corresponding author, Assistant Professor, E-mail: dkumar.mech@mnit.ac.in
[a] Ph.D. Student, E-mail: ashish.memech@gmail.com

 ISSN: 1229-9367 (Print), 1598-6233 (Online)

(2000) and Liu and Chen (2003a) reported that by adding only a few percentage (by weight/volume) of CNTs in a matrix material, the stiffness and strength of a resulting composite can increase significantly. Many investigators have demonstrated the mechanical load carrying capacities of CNTs in nanocomposites through their experimental work (Bower *et al*. 1999; Qian *et al*. 2000) and numerical simulations (Liu and Chen 2003a, b).

In 2007, the research article 'The Rise of Graphene' by Geim and Novoselov (2007) fetched the attention of researchers worldwide into a new window of nanoscience. Graphene, a basic structural unit of some carbon allotropes such as graphite, CNTs, and fullerenes, is a monolayer of sp^2-hybridized carbon atoms packed in a two-dimensional honeycomb crystal lattice. Owing to high surface area, aspect ratio, tensile strength, thermal conductivity and electrical conductivity associated with low coefficient of thermal expansion and production cost, graphene is preferred over other conventional nanofillers, including CNT, carbon nanofillers (CNF), expanded graphite (EG) (Sakhaee-Pour 2009, Zhu *et al*. 2010, Kuilla *et al*. 2010). One possible route to harnessing these peculiar properties of graphene for various applications would be to make nanocomposites based on graphene sheets. Pott's *et al*. (2011) reviewed the graphene reinforced polymer nanocomposites and highlighted its potential applications and challenges. In some of the studies, it is also reported that the improvement in mechanical and electrical properties of graphene-based nanocomposites are much better in comparison to that of other carbon filler-based nanocomposites (Stankovich *et al*. 2006, Kim and Macosko 2009). Further, the 2D structure of graphene with the higher surface-to-volume ratio is more favourable for sensor structure and catalytic performance than CNTs (Xu *et al*. 2008).

At the nanoscale, analytical models are either difficult to establish or too complicated to solve. At the same time, there are enormous challenges in the experimental development and characterizations of CNT- and graphene-based nanocomposites (Bower *et al*. 1999, Qian *et al*. 2000, Potts *et al*. 2011) because of difficult and expensive processes involved. Therefore, cost-effective and less time-consuming computational approaches play a significant role in the development and characterization of CNT- and graphene-based nanocomposites to provide simulation results for better understanding, analysis and design of such nanocomposites. Presently, two computational approaches based on molecular dynamics (MD) approach and continuum mechanics approach for smaller and larger time and length scales, respectively, are used for characterizing individual CNT/graphene as well as nanocomposites. At the same time, purposes of simulations would also fix the approach to be used. For instance, for local response prediction, such as interactions among individual atoms, or chemical reactions between the CNT and a matrix material, MD simulation should be adopted, whereas for the global responses of individual CNTs and CNT-based composites, the continuum mechanics approach should be applied (Liu and Chen 2003a).

There are many investigations on applications of MD approach for simulation of individual CNTs/graphenes or nanocomposites for understanding their behaviour and hence, providing some initial guidelines to the experimental work. Al-Ostaz *et al*. (2008) carried out the MD simulations to estimate the elastic properties of the single-walled nanotube (SWCNT), interfacial bonding, polyethylene matrix and composites with aligned and randomly distributed SWCNTs. The elastic behaviour of polymeric nanocomposites was investigated by Cho and Sun (2007) using molecular dynamics simulations to study the inclusion size effect on polymeric nanocomposites. Bu *et al*. (2009) have investigated the mechanical behaviour of graphene nanoribbons by MD simulations. An atomistic simulation method was adopted by Sakhaee-Pour (2009) to investigate the elastic characteristics of the defect-free single layered graphene sheet. Tsai and Tu (2010) have computed

the mechanical properties of graphite in the forms of single graphene layer and graphite flakes using MD simulation. Zhang *et al*. (2014) studied the load transfer of graphene/carbon nanotube/polyethylene hybrid nanocomposite by molecular dynamics simulation.

Although molecular simulations have been broadly used in modeling reinforced polymer nanocomposites, but limited to small molecular systems simulated over a limited time which hinder MD simulations to study the effect of fiber sizes and orientations on the mechanical behavior of reinforced polymer nanocomposites. In order to overcome the limitations of MD simulations, coarse-grained (CG) models have also been developed in the literature (Rzepiela *et al*. 2011). CG models result in substantial increase in the accessible time and length scales while partially retaining the molecular details of an atomistic system, by mapping a set of atoms to a CG bead. Using a coarse-grained (CG) model Arash *et al*. (2015) studied the tensile fracture behavior of short CNT reinforced poly (methyl methacrylate) (PMMA) matrix composites. Mousavi *et al*. (2016) developed a CG model of cross linked carbon nanotube (CNT) reinforced polymer matrix composites. Very lately, a CG model for predicting the J-integral of carbon nanotube (CNT)/polymer composites is proposed by Arash *et al*. (2016). The distinguishing feature of the developed model is the calculation of J-integral without the need of information about the crack tip, which makes it applicable to complex polymer systems.

The mechanical properties of a certain polymer nanocomposite system may be affected by multiple uncertain parameters such as the volume fraction, aspect ratio, curvature and stiffness of reinforcement, and stiffness of the matrix. Therefore, it is required to treat these input parameters as stochastic variables. Vu-Bac *et al*. (2015a) proposed a stochastic analysis to predict bulk properties like Young's and shear modulus of fully exfoliated Polymeric nanocomposites (PNCs) by considering the clay weight content, clay platelets aspect ratio, and the energy release rate of the epoxy as stochastic input parameters. Vu-Bac *et al*. (2015b) proposed a stochastic multiscale method to quantify the correlated key-input parameters influencing the mechanical properties of polymer nanocomposites (PNCs). Ghasemi *et al*. (2014) optimized the CNT content in generic nanocomposite solids by considering CNT parameters (i.e., length, waviness, agglomeration, orientation and dispersion) as random variables and estimated the number of CNTs into a resin to design an optimal and reliable structural component. To overcome the computational cost in stochastic optimization problems, Ghasemi *et al*. (2015) presented an efficient sequential algorithm to determine the optimal volume fraction of fiber and its distribution in structures made of composite materials.

The continuum mechanics approach has also been applied for simulating the mechanical and thermal responses of individual CNTs/graphenes or CNT-based nanocomposites (Aydogdu 2014, Semmah *et al*. 2014). For simulating individual CNTs using continuum approach, they are treated as beams, shells or solids in cylindrical shapes (Wong 1997, Sohlberg *et al*. 199 8, Ru 2001). Such as using single elastic beam model, Besseghier *et al*. (2015) investigated the nonlinear free vibration analysis of embedded zigzag CNT. The effective mechanical properties of CNT-based composites was evaluated by Liu and Chen (Liu and Chen 2003a, Chen and Liu 2004) using a 3D nanoscale representative volume element (RVE) based on continuum mechanics and using the finite element method (FEM). Analytical formulations were presented by Shokrieh and Rafiee (2010a) to predict the elastic moduli of graphene sheets and carbon nanotubes using a linkage between molecular lattice structure and equivalent discrete frame structure based on nanoscale continuum mechanics approach. Joshi and Upadhyay (2014) used the continuum mechanics model to evaluate the elastic properties of multi-walled carbon nanotube reinforced composite.

Moreover, there have been many issues in CNT/graphene-based nanocomposites, e.g., bonding

(i.e., interface) between the nano-fillers and the matrix, dispersion and alignment of nano-fillers into the matrix, and defects such as waviness of CNT/graphene which would have significant effects on various properties of these nanocomposites and hence, are very important from practical points of view. Joshi *et al*. (2011) studied the effects of pinhole defects on mechanical properties of wavy CNT-based nanocomposites using 3D representative volume element with long carbon nanotubes and observed that waviness of CNT significantly reduces the effective reinforcement of the nanocomposites. Li and Chou (2009) studied the failure of CNT/polymer composites using micromechanics and finite element simulation and investigated the effects of nanotube waviness, and random nanotube distribution relative to aligned straight nanotubes are investigated. They concluded that the nanotube waviness tends to reduce the elastic modulus but increase the ultimate strain of a composite. The tensile behaviour of an embedded CNT in the polymer matrix in the presence of van der Waals interactions was studied by Shokrieh and Rafie (2010b) using finite element method. Qian *et al*. (2000) found that because of the tendency of CNTs to agglomerate and to bundle together into the polymer matrices, many defects sites are created in the nanocomposites that result in limiting the efficiency of the nanocomposite. Salvetat *et al*. (1999) investigated the effect of dispersion of CNTs on the mechanical properties of polymer/CNT composites to conclude that poor dispersion and rope-like entanglement of CNTs led to a drastic weakening of the resulting nanocomposites.

From the above literature study, it is manifested that there have been many simulations studies on the application of MD and Continuum mechanics approaches separately for the characterization of nano-fillers based composites. The preferred approach for simulations of nano-fillers, such as CNT/graphene, based composites should be a multiscale approach (i.e., integrating the MD and continuum mechanics approaches) which account for the physics at nanoscales and at the same time, efficient enough to handle nanocomposites at larger length scales. The development of such a multiscale approach for simulations of nanoscale materials is in early stage of its growth, so the prevailing MD and continuum mechanics (based on FEM) approaches are still the feasible approaches for conducting some preliminary studies of such materials. At the same time, using semi-concurrent multiscale methods, as developed by Talebi *et al*. (2014) and used by Silani *et al*. (2014), it is possible to couple two different software packages, e.g., MD software with a FE software.

As evident from the above literature survey, there are very few studies on the mechanical behavior of graphene sheet reinforced nanocomposite and its comparison with CNT reinforced nanocomposite to investigate the effect of shape of reinforcement (such as cylindrical and plate shapes of CNT and graphene, respectively) on the elastic properties of aligned nanofiller nanocomposites. To the best of author's knowledge, none of the studies are found in literature based on the elastic properties of graphene reinforced nanocomposite using the method of representative volume element through finite element methods. Therefore the aim of this paper is to evaluate and compare the effective elastic properties of CNT- and graphene-based nano-composites using a 3-D nanoscale representative volume element (RVE) based on continuum mechanics. Various elastic properties of CNT- and graphene-reinforced nanocomposites are evaluated from finite element method (FEM) analysis of the square RVE by applying periodic displacement boundary conditions for different loading cases. The FEM analysis of RVE is carried out using the commercial FEM based package COMSOL Multiphysics. The effects of the matrix material, the volume fraction and the length of reinforcements in RVE on the response of nanocomposites in terms of change in their elastic properties are studied. Results are validated by comparing the finite element based predictions of the elastic properties of the CNT-based

nanocomposite obtained in the present study with the results predicted by analytical and/or semi empirical approaches (i.e., rules of mixtures and Halpin-Tsai model), and the available results in the literature. The present study is limited to the defect-free nanocomposites with perfectly straight CNT/flat graphene distributed in a periodic pattern within the matrix with the perfect interface in between.

2. Representative volume element (RVE)

In a nanocomposite specimen, the nanofillers i.e., CNTs/graphenes are randomly distributed throughout the volume. To simplify the simulations of mechanical responses of these nanocomposites under the assumption that CNTs/graphenes are distributed throughout the matrix in a periodic pattern in square-packed array, the concept of unit cells with periodic boundary

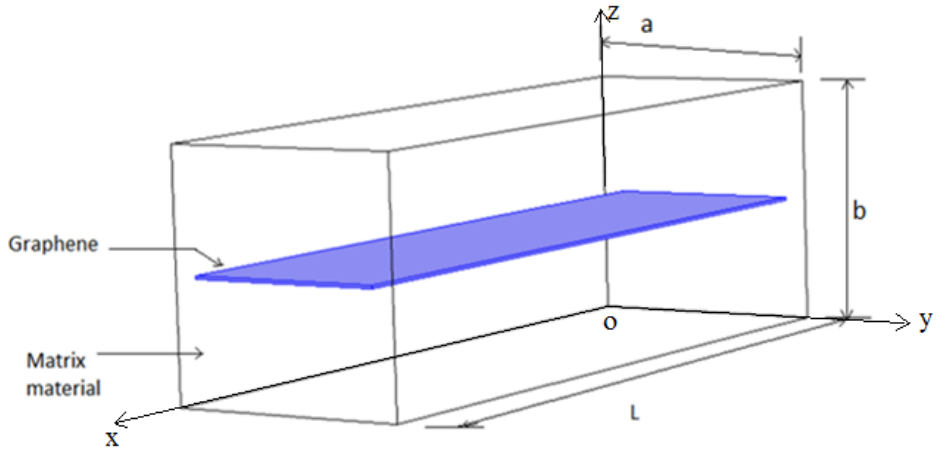

(a)

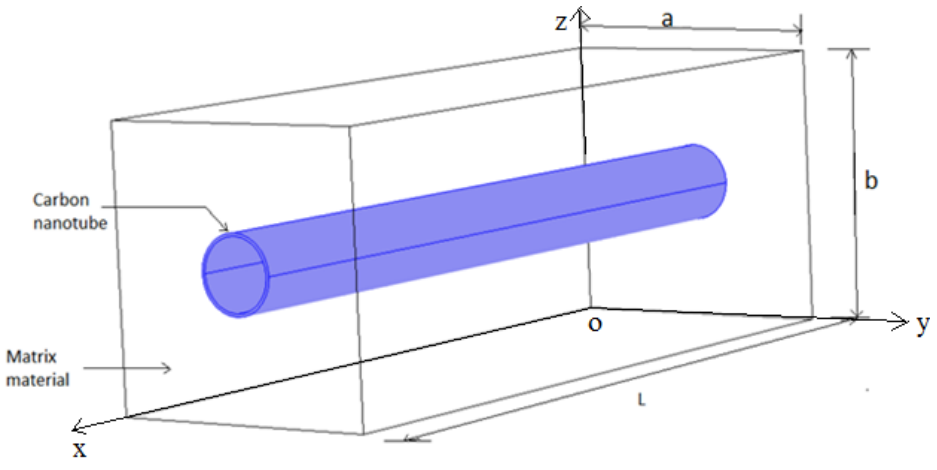

(b)

Fig. 1 Square RVE showing (a) graphene reinforced in matrix; (b) CNT reinforced in matrix

conditions, also known as representative volume elements (RVE) (Sun and Vaidya 1996, Segurado *et al*. 2003), as applied successfully in the studies of conventional fiber-reinforced composites at the micro scale is extended to study the mechanical responses of CNT- and graphene-based composites at nanoscale (Hyer 1998). This periodic distribution of nanofillers in a matrix material also represents a special case of alignment of CNT/Graphene in matrix material (Kondo *et al*. 2008, Wang *et al*. 2008). In this paper nanoscale square RVE based on the 3-D elasticity theory proposed in Ref. (Liu and Chen 2003b) and having the same elastic constants and volume fraction as that of the nanocomposite is used to calculate the effective properties of CNTs/graphenes reinforced nanocomposites (Refer Fig. 1).

3. Periodic boundary conditions on RVE

It is very paramount to impose correct boundary conditions on the RVE in the effective evaluation of elastic moduli. Boundary conditions on the RVE should be such that they simulate the actual deformation within the nanocomposite under a given loading condition. In the present analysis, the boundary conditions on the RVE for various loading conditions, as derived by Sun and Vaidya (1996) by judicious use of symmetry and periodicity conditions and used for the prediction of mechanical properties of the conventional composite from RVE approach, are utilized and applied to the finite element model. Following subsections contain the displacement boundary conditions applied to the finite element model for normal loading, transverse shear loading, and longitudinal shear loading cases to calculate various elastic moduli.

3.1 Boundary conditions for normal loading

Following periodic displacement boundary conditions on the RVE are applied to calculate longitudinal and transverse modulus and Poison's ratios:

3.1.1 For calculating E_1, u_{12} and u_{13} (refer Fig. 2)

$$u_{11}(0,y,z)=u_{22}(x,0,z)=u_{33}(x,y,0)=0;u_{11}(L,y,z)=\delta_1 \tag{1}$$

where u_{11}, u_{22} and u_{33} represent displacement components in x, y and z directions, respectively, and δ_1 is the constant value of displacement applied in the x-direction on $x = L$ face of the RVE.

3.1.2 For calculating E_2 and u_{23}

$$u_{11}(0,y,z)=u_{22}(x,0,z)=u_{33}(x,y,0)=0;u_{22}(x,a,z)=\delta_2 \tag{2}$$

where δ_2 is the constant value of displacement applied in the y-direction on $y = a$ face of the RVE.

3.1.3 Similarly, for calculating E_3

$$u_{11}(0,y,z)=u_{22}(x,0,z)=u_{33}(x,y,0)=0;u_{33}(x,y,b)=\delta_3 \tag{3}$$

where δ_3 is the constant value of displacement in the z-direction on $z = b$ face of the RVE.

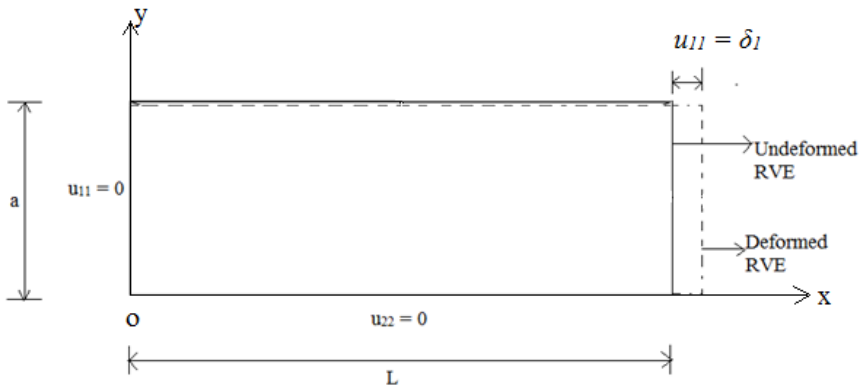

Fig. 2 Typical RVE under normal loading in x-direction (for calculating E_1, υ_{12} and υ_{13})

3.2 Boundary conditions for transverse shear loading

3.2.1 For calculating G_{23} (refer Fig. 3)

$$u_{11}(x,y,0) = u_{22}(x,y,0) = u_{33}(x,y,0) = 0; u_{22}(x,y,b) = \delta_t \tag{4}$$

where δ_t is the constant value of displacement in y-direction on $z = b$ face of the RVE, as shown in Fig. 3.

3.3 Boundary conditions for longitudinal shear loading

3.3.1 For calculating G_{12} (refer Fig. 4)

$$u_{11}(x,0,z) = u_{22}(x,0,z) = u_{33}(x,0,z) = 0; u_{11}(x,a,z) = \delta_l \tag{5}$$

where δ_l is the constant value of displacement in the x-direction on $y = a$ face of the RVE, as shown in Fig. 4.

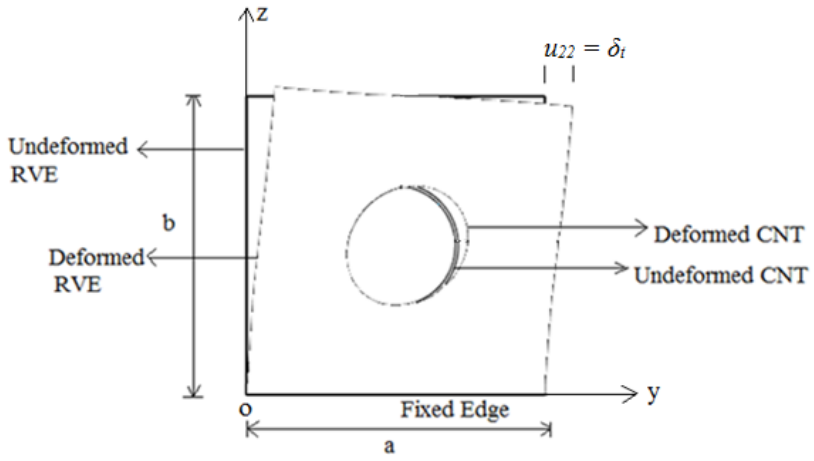

Fig. 3 RVE under transverse shear loading (for calculating G_{23})

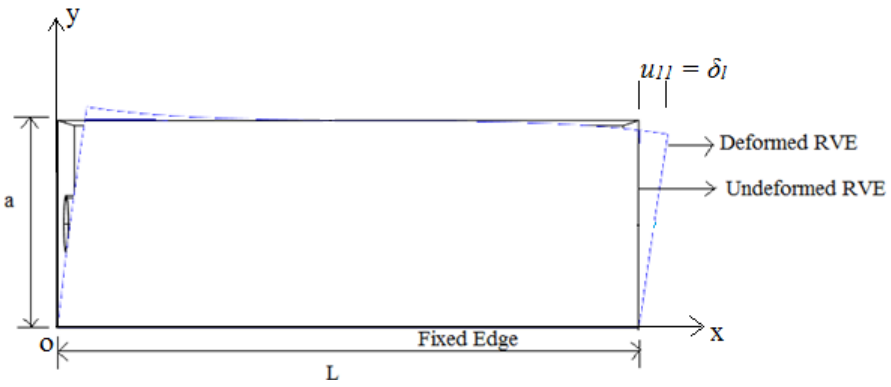

Fig. 4 RVE under longitudinal shear loading (for calculating G_{12} and G_{13})

3.3.2 Similar to G_{12}, the boundary conditions for calculating G_{13} would be as follows

$$u_{11}(x,y,0)=u_{22}(x,y,0)=u_{33}(x,y,0)=0;u_{11}(x,y,b)=\delta_l \tag{6}$$

where δ_l is the constant value of displacement in the x-direction on $z = b$ face of the RVE.

4. Homogenization method for evaluating average stress and strain over the RVE

At the nanoscale, the RVE representing a matrix reinforced with CNT/graphene system is actually a heterogeneous composite medium which is to be used for evaluating effective (i.e., average) material properties of the nanocomposite that is considered to be homogeneous at larger scales (i.e., micro and meso scales). Therefore, it is required to use some homogenization techniques to find a globally homogeneous medium equivalent to the original heterogeneous composite medium at the nanoscale and to reduce the non-homogeneous stress and strain fields within the heterogeneous material obtained from the finite element analysis of RVE to the volume-averaged stress and strain. Following paragraphs contains homogenization procedure to determine the effective moduli that describe the 'average' material properties of the actual heterogeneous nanocomposite.

The heterogeneous models of nanocomposite reinforced with CNT and graphene are shown in Fig. 1. using square RVE. The interface between two phases (i.e., matrix and reinforcement) in the RVE is assumed to be perfect. Individual phases have isotropic material properties, and it is assumed that the constitutive law in the matrix and the reinforcement is given by the following generalized Hooke's Law, written in summation convention

$$\sigma_{ij}=C_{ijkl}\varepsilon_{kl} \qquad i,j,k,l=1,2,3 \tag{7}$$

where σ_{ij}, ε_{kl} and C_{ijkl} are the components of the stress tensor, the linear strain tensor and the stiffness tensor, respectively.

The finite element analysis (FEA) of the RVE would yield the above-mentioned stress and strain fields within the heterogeneous material. The effective (i.e., averaged) stiffness coefficients

of nanocomposite (at micro or macro scale) can be calculated from

$$\overline{\sigma_{ij}} = C^{e}_{ijkl}\,\overline{\varepsilon_{kl}} \tag{8}$$

where C^{e}_{ijkl} refers to the effective stiffness tensor, and $\overline{\sigma_{ij}}$ and $\overline{\varepsilon_{kl}}$ are the volume-averaged stress and strain tensors calculated over the volume of the RVE using following volumetric integral expressions as

$$\overline{\sigma_{ij}} = \frac{1}{V_{RVE}} \int_{V_{RVE}} \sigma_{ij}(x,y,z)dV \tag{9}$$

$$\overline{\varepsilon_{kl}} = \frac{1}{V_{RVE}} \int_{V_{RVE}} \varepsilon_{kl}(x,y,z)dV \tag{10}$$

where C^{e}_{ijkl} refers to the effective stiffness tensor, and $\overline{\sigma_{ij}}$ and $\overline{\varepsilon_{kl}}$ are the volume-averaged stress and strain tensors calculated over the volume of the RVE using following volumetric integral expressions as

$$C^{e}_{ijkl} = \frac{\overline{\sigma_{ij}}}{\overline{\varepsilon_{kl}}}, \quad i=j=k=l; \quad (\text{for pure normal strain states}) \tag{11}$$

$$C^{e}_{ijkl} = \frac{\overline{\sigma_{ij}}}{2\overline{\varepsilon_{kl}}}, \quad (i=k)\neq(j=l); \quad (\text{for pure shear strain states}) \tag{12}$$

The Poison's ratios are given by

$$\nu_{ij} = -\frac{\overline{\varepsilon_{jj}}}{\overline{\varepsilon_{ii}}} \tag{13}$$

Therefore, Eqs. (11)-(13) are used, respectively, to calculate the effective Young's moduli, shear moduli and Poison's ratios of the nanocomposite.

5. Analytical and semiempirical approaches used for validation

In this section analytical and semiempirical approaches used for validation of the procedure based on finite element analysis using COMSOL and followed in the present study are described. Under the assumption of perfect bonding between the reinforcement and the matrix, following relationships based on mechanics of materials, called rules of mixtures are used to calculate the properties of the RVE.

$$E_1 = V_f E_f + (1-V_f)E_m \tag{14}$$

$$E_2 = \frac{E_f E_m}{E_m V_f + (1-V_f)E_f} \tag{15}$$

$$G_{12} = \frac{G_f G_m}{G_m V_f + G_f (1 - V_f)} \tag{16}$$

$$\nu_{12} = \nu_f V_f + \nu_m (1 - V_f) \tag{17}$$

In Eqs. (14)-(17), subscripts '*m*' and '*f*' correspond to the matrix and the reinforcement (i.e., CNT), respectively, and accordingly *E*, *G* and υ denote the Young's modulus, shear modulus and Poisson's ratio of matrix/reinforcement, respectively; V_f is the volume fraction of CNT reinforced in the RVE given by

$$V_f = \frac{V_{CNT}}{V_{RVE}} = \frac{\pi(r_0^2 - r_i^2) L_{CNT}}{(ab - \pi r_i^2) L} \tag{18}$$

where r_o and r_i are the external and internal radii of the CNT, respectively; *a* and *b* are the cross-sectional dimensions of the RVE and for square RVE *a* = *b*, and; L_{CNT} and *L* represent the lengths of CNT and RVE, respectively. For full-length CNT reinforced in the matrix, $L_{CNT} = L$.

The rules of mixtures is preferred over other approaches, such as numerical, semi-empirical, experimental, because of its simplicity, but its predictions are adequate for verifying the results for effective Young's modulus in the CNT axial direction i.e., E_1 (Hyer 1998). In addition to rules of mixtures, Halpin-Tsai (HT) model which involve semiempirical relationships obtained by curve fitting to the exact results based on elasticity is also used to compare the average properties of CNT-reinforced RVE. Halpin-Tsai model provides a better approximation of transverse modulus than rules of mixtures because of consideration of reinforcement geometry, packing geometry and loading condition (Halpin 1969). For axial modulus, HT model reduces to rules of mixtures (i.e., Eq. (14)), and for transverse modulus, it provides the following relationships.

$$\frac{E_2}{E_m} = \frac{1 + \xi \eta V_f}{1 - \eta V_f}, \quad \text{where} \quad \eta = \frac{E_f - E_m}{E_f + \xi E_m} \tag{19}$$

where ξ is reinforcing factor which depends on upon reinforcement geometry, packing geometry and loading condition. For a reinforcement of circular cross-section in a packing geometry of square array, $\xi = 2$.

Similarly, for in-plane shear modulus

$$\frac{G_{12}}{G_m} = \frac{1 + \xi \eta V_f}{1 - \eta V_f}, \quad \text{where} \quad \eta = \frac{G_f - G_m}{G_f + \xi G_m} \tag{20}$$

wherein the value of reinforcing factor, $\xi = 1$ for reinforcement of circular cross-section in a packing geometry of square array.

6. Verification of results

To verify the procedure followed, the finite element predictions of the elastic constants of CNT reinforced nanocomposite obtained in the present study are compared with the results predicted by

Table 1 Elastic modulii (in GPa) of CNT reinforced square RVE ($V_f = 0.04871$)

Elastic constants	FEM	ROM	H-T	Ref. (Liu and Chen 2003b)	Ref. (Joshi and Upadhyay 2014)
E_1	238.9679	238.9680	238.9680	238.9600	238.3886
E_2	222.5916	208.1100	217.1787	234.7400	-
G_{12}	88.5112	80.0184	82.0626	-	-
v_{12}, v_{13}	0.3000	0.3000	0.3000	0.3000	0.2887
v_{23}	0.3284	-	-	0.4204	-

analytical and semiempirical approaches, i.e., rules of mixtures and Halpin-Tsai (H-T) model (as described in Section 5), and the available results in the literature (Liu and Chen 2003b, Joshi and Upadhyay 2014). A square RVE ($a = b = 17.724$ nm) having CNT (single-walled) reinforced in a matrix with volume fraction $V_f = 0.04871$ of the following dimensions and properties is considered for the comparison.

For matrix: Length $L = 100$ nm, Young modulus $E_m = E_f/5$, Poisson's ratio, $\upsilon = 0.3$.
For CNT: Length $L = 100$ nm, Young modulus $E_f = 5E_m$,
Poisson's ratio, $\upsilon = 0.3$, outer radius $r_o = 5$ nm, inner radius $r_i = 4.6$ nm.

The finite element mesh model of a square RVE reinforced with CNT is shown in Fig. 5. The results of comparison between elastic constants predicted using finite element procedure of the present study and with those evaluated from rules of mixtures, Halpin-Tsai model and reported results in Refs. (Liu and Chen 2003b, Joshi and Upadhyay 2014) are given in Table 1. It can be noticed from Table 1 that in general, a good agreement can be observed between the finite element predictions of elastic moduli and those calculated from the analytical and semiempirical approaches as well as the available results in the literature (Liu and Chen 2003b, Joshi and Upadhyay 2014). This comparison verifies the accuracy of the procedure followed in this study for a complete nanomechanical analysis of graphene as well as CNT-reinforced nanocomposites.

7. Present study

To evaluate the effective material constants of CNT- and graphene-based nanocomposites, the square RVE (Fig. 1) containing CNT or graphene in a matrix is studied using FEM-based tool COMSOL Multiphysics. A square RVE of CNT/graphene reinforced in a matrix nanocomposite with volume fraction V_f is considered. The dimensions and elastic properties of the matrix, the CNT, and the graphene materials are given below.

For matrix: Length $L = 100$ nm, Young modulus $E_m = 10$ to 500 GPa, Poisson's ratio $\upsilon = 0.3$.
For CNT: Length $L_{CNT} = 100$ nm (for long CNT) and $L_{CNT} = 50$ nm (for short CNT),
Thickness of CNT $t = 0.4$ nm, Young modulus E_f (CNT) = 1 TPa,
Poisson's ratio $\upsilon = 0.3$, outer radius $r_o = 5$ nm, inner radius $r_i = 4.6$ nm.
For graphene: Length $L_{graphene} = 100$ nm (for long graphene) and
$L_{graphene} = 50$ nm (for short graphene), Thickness of graphene, $t = 0.4$ nm,
Young modulus E_f (graphene) = 1 TPa, Poisson's ratio $\upsilon = 0.3$.

The volume fraction of CNT reinforced nanocomposite is given by Eq. (18). For the given dimensions of CNT and volume fraction V_f, cross-sectional dimensions of the square RVE can be evaluated from the same equation.

The volume fraction of graphene-reinforced nanocomposite is given by

$$V_f = \frac{V_{graphene}}{V_{RVE}} = \frac{wtL_{graphene}}{abL} \tag{21}$$

where a and b are the cross-sectional dimensions of the RVE (for square RVE $a = b$), w is the width of the graphene which is taken as $0.8a$.

For the given dimensions of graphene and volume fraction V_f, cross-sectional dimensions of the square RVE can be evaluated from Eq. (21).

The RVE is meshed with tetrahedron elements using physics-controlled meshing feature of COMSOL with fine enough mesh near to CNT/graphene (as shown in Figs. 5 and 6) to deliver converged FEM results. Various periodic boundary displacement conditions for different loading cases, as discussed in Section 3 and shown in Figs. 2-4, are applied to yield the stress and strain fields within the actual heterogeneous RVE. The corresponding average quantities ($\bar{\sigma}_{ij}$ and $\bar{\varepsilon}_{ij}$) are obtained by taking the volumetric integral of stresses and strains, as given by Eqs. (9) and (10). By using the calculated values of average stress and average strain, the effective nanocomposite moduli can be evaluated using Eqs. (11)-(13) as the ratio of average stress (or average transverse strain, for Poisson's ratio) to the average strain.

In this paper, an initial study is conducted to compare the elastic constants of CNT and graphene reinforced nanocomposites for $E_f/E_m = 5$ and volume fraction $V_f = 0.04871$. For the same volume fraction, graphene- and CNT-reinforced in different matrix materials (with E_f/E_m varying from 2 to 100) are also looked into to investigate the response of nanocomposite in terms of variations in its stiffness properties. Moreover, the effect of volume fraction (varying from 1% to 10%) on elastic stiffness constants of CNT and graphene reinforced nanocomposites is also investigated. Finally, a comparison of elastic properties of nanocomposites embedded with 1% of long (i.e., graphene/CNT running through the RVE length) and short (i.e., graphene/CNT of half of the RVE length placed centrally) reinforcements is made.

8. Results and discussions

Various elastic properties of CNT- and graphene-reinforced in a matrix material (with E_f / E_m = 5) are evaluated from FEM analysis of a 3D nanoscale square RVE by applying periodic boundary displacement conditions for different loading cases (refer Section 3 and Figs. 2-4 for volume fraction V_f of 4.871%. Results of elastic properties of CNT and graphene-based nanocomposites are listed in Table 2.

It is to bring in the notice that in the following discussion the comparison of elastic properties of the CNT and the graphene reinforcements is made with reference to the corresponding properties of the pure matrix material. From Table 2, it can be noted that CNT and graphene reinforced nanocomposites show transversely isotropic and orthotropic behaviour, respectively. The results also show that all stiffness properties are increased by the inclusion of CNT as well as graphene as nano-scale fillers in the matrix. Increase in stiffness in the axial direction (i.e., E_1) as compared to matrix material is almost same for CNT and graphene reinforcements and the

Table 2 Comparison of Elastic constants for CNT and graphene reinforced nanocomposites (for $E_f / E_m = 5$ and V_f 0.04871)

Elastic constants (GPa)	CNT based nanocomposite	Graphene based nanocomposite
E_1	238.9679	238.9680
E_2	222.5916	230.9305
E_3	222.5916	213.8684
G_{12}	88.5112	89.4098
G_{23}	92.5559	80.7915
G_{13}	88.5112	80.2993
v_{12}	0.3000	0.2999
v_{23}	0.3284	0.3037
v_{13}	0.3000	0.2999

increase is nearly 19.5%. Transverse modulus E_2 along the width direction (i.e., *y*-axis) of graphene is also increased by 15.5% as compared to the pure matrix, and this increase is more than the corresponding increase (i.e., 11.3%) in the case of the CNT-based nanocomposite. So, the graphene reinforcement in nanocomposites provides better bi-directional stiffening effects than CNT reinforcement which can be attributed to the biaxial stiffness properties of the 2-D graphene sheet. The observation for the transverse modulus E_3 along the thickness direction (i.e., *z*-axis) of graphene is in contrast to E_2 i.e., for CNT nanocomposite the increase in E_3 (i.e., 11.3%) is more than the corresponding increase of nearly 7% in the case of the graphene-based nanocomposite. The effects of reinforcement types on shear moduli can also be observed from Table 2. The in-plane (*xy*-plane) shear modulus G_{12} is increased by 16.3% in the case of graphene reinforcement which is slightly more than the corresponding increase of 15.1% in the case of CNT nanocomposite. A significant difference in the values of shear moduli in transverse planes (i.e., G_{23} and G_{13}) between the CNT and the graphene-based nanocomposites can also be noticed. CNT reinforcement is found to provide better shear properties in transverse planes than graphene reinforcement, as evident from Table 2. Not much difference in the values of Poisson's ratios in various planes is observed for the two types of reinforcements, except υ_{23} in the case of CNT nanocomposite which is increased substantially.

The effects of variation in the matrix material (represented in terms of E_f / E_m ratio) on normalized (with respect to E_m) values of the extensional and the shear moduli of CNT- as well as graphene-reinforced nanocomposites for the volume fraction of 0.04871, are listed in Tables 3 and 4, respectively. Some of the results for E_1 / E_m reported in the literature (Liu and Chen 2003b, Joshi and Upadhyay 2014) are also provided in Table 3 for validation purpose. To better visualize the effect of variation in E_f / E_m on various elastic stiffness properties of the nanocomposite, the normalized values presented in Tables 3 and 4 are also plotted, respectively, in Figs. 7 and 8. It is important to note that the different matrix materials considered, with E_f / E_m = 2, 5, 10, 15, 20, 40 and 100, represent a range of matrix material with stiffness varying from ceramic to polymer, including metal.

It can be observed from Table 3 and Fig. 7 that with the increase in E_f / E_m ratio (i.e., matrix material becoming less stiff as compared to CNT/graphene material), values of all normal elastic moduli of CNT as well as graphene nanocomposites are increased by varying amount, and this increase is very substantial for axial modulus (i.e., E_1), for both types of reinforcement. Fig. 7 also

Table 3 Normalized effective extensional modulii of CNT- and graphene-reinforced nanocomposites with different matrix materials (for $V_f = 0.04871$)

E_f/E_m	CNT Nanocomposites				Graphene Nanocomposites		
	E_1/E_m						
	Present Study	Ref. (Liu and Chen 2003b)	Ref. (Joshi and Upadhyay 2014)	$E_2/E_m = E_3/E_m$	E_1/E_m	E_2/E_m	E_3/E_m
2	1.0487	-	-	1.0382	1.0487	1.0455	1.0305
5	1.1948	1.1948	1.1919	1.1130	1.1948	1.1546	1.0693
10	1.4383	1.4384	1.4316	1.1813	1.4383	1.2814	1.1018
15	1.6818	-	1.6712	1.2216	1.6819	1.3691	1.1216
20	1.9254	-	-	1.2491	1.9254	1.4338	1.1355
40	2.8996	-	-	1.3080	2.8996	1.5831	1.1658
100	5.8221	-	5.7457	1.3677	5.8222	1.7319	1.1945

Note: E_f is the Young's modulus of reinforcement material (graphene or CNT)

reveals that change in the normalized values of E_1 for CNT and graphene-based nanocomposites with the change in matrix stiffness follow a similar trend. It is also important to note from Table 3 and Fig. 7 that irrespective of E_f/E_m ratio, the transverse in-plane stiffness (i.e., E_2) of graphene nanocomposite is more than that of CNT nanocomposite, but the reverse is true for the transverse out-of-plane stiffness (i.e., E_3).

From Table 4 and Fig. 8, it can be mentioned that effect of matrix material on shear moduli of the CNT-based nanocomposite is not very significant. This is also true for the shear moduli of graphene nanocomposite in transverse planes (i.e., 1-3 and 2-3 planes). On the contrary, it is interesting to note that the effect of matrix materials on the in-plane shear modulus (i.e., G_{12}) of graphene nanocomposite is very significant. The values of G_{12} for graphene nanocomposite show an increasing trend with the increase in E_f/E_m ratio and it is more than the corresponding values for CNT nanocomposite.

Table 4 Normalized effective shear modulii of CNT- and graphene-reinforced nanocomposites with different matrix materials (for $V_f = 0.04871$)

E_f/E_m	CNT nanocomposites		Graphene nanocomposites		
	G_{23}/G_m	$G_{12}/G_m = G_{13}/G_m$	G_{12}/G_m	G_{13}/G_m	G_{23}/G_m
2	1.0132	1.0093	1.0462	1.0260	1.0303
5	1.0341	1.0306	1.1623	1.0438	1.0502
10	1.0483	1.0531	1.3059	1.0504	1.0574
15	1.0550	1.0673	1.4103	1.0528	1.0600
20	1.0589	1.0769	1.4897	1.0539	1.0614
40	1.0661	1.0972	1.6793	1.0557	1.0637
100	1.0730	1.1150	3.7526	1.0569	1.0657

Note: E_f is the Young's modulus of reinforcement material (Graphene or CNT)

Table 5 Comparison of elastic properties of long and short CNT- and graphene- reinforced nanocomposites (for $E_f/E_m = 5$ and $V_f = 0.01$)

Elastic constants	CNT nanocomposite (Short)	CNT nanocomposite (Long)	Graphene nanocomposite (Short)	Graphene nanocomposite (Long)
E_1 (GPa)	208.0000	208.0055	207.4077	208.0000
E_2 (GPa)	204.4612	204.8704	206.9679	207.3091
E_3 (GPa)	204.4612	204.8704	202.9586	203.0465
G_{12}(GPa)	79.6704	79.2845	79.9556	79.7989
G_{23}(GPa)	79.3881	79.5497	77.6922	77.6664
G_{13}(GPa)	79.6704	79.2845	77.6605	77.5565
v_{12}	0.2981	0.3000	0.2996	0.2999
v_{23}	0.3077	0.3095	0.3005	0.3004
v_{13}	0.2981	0.3000	0.3001	0.2999

Note: E_f is the Young's modulus of nano-filler material (Graphene or CNT)

A comparison of elastic properties of the CNT and the graphene reinforced nanocomposites is also made for various volume fractions (varying from 1% to 10%) of the reinforcement. The effect of the change in volume fraction of reinforcements (i.e., CNT and graphene) inside the matrix material (with $E_f/E_m = 5$) on the elastic properties of the resulting nanocomposite is plotted in Figs. 9 (a-f). It can be noted from Figs. 9(a)-(f) that theoretically all elastic properties of CNT, as well as graphene, reinforced nanocomposite increase with the increase in the volume fraction. For all volume fractions, there is no difference in the axial stiffness (i.e., E_1) of the CNT and the graphene reinforced nanocomposites, and the increase in the value of E_1 (for 10% reinforcement) is very significant (about 40%), refer Fig. 9(a). Besides axial stiffness, it can also be seen from Figs. 9(b) and 9(d) that irrespective of the amount of reinforcement, graphene improves other in-plane stiffness properties (i.e., E_2 and G_{12}) as well better than CNT. On the other hand, Figs. 9(c), (e) and (f) show that because of poorer out-of- plane stiffness properties (i.e., E_3, G_{13}, and G_{23}) of graphene than CNT, the resulting graphene-based nanocomposite would also have inferior out-of-plane stiffness properties than CNT based-nanocomposite, for all values of volume fractions. It is also important to note that effect of volume fraction on the shear moduli in transverse planes (i.e., G_{23} and G_{13}) is less significant for graphene nanocomposite and this observation is in contrast to CNT-reinforced nanocomposites. Altogether, Figs. 9(a)-(f) also depict that irrespective of volume fraction, CNT-based nanocomposites provide overall good stiffness properties in all directions and planes as compared to graphene nanocomposite.

Table 5 depicts the comparison of elastic properties of long and short CNT- and graphene-reinforced nanocomposites for $E_f/E_m = 5$ and $V_f = 0.01$. It can be noticed from Table 5 that for the same volume fraction (i.e., 1%), long nanofiller (graphene as well as CNT) results in slight increase in the normal elastic moduli (E_1, E_2, and E_3) of the resulting nanocomposites as compared to the short length reinforcement. This finding of more effectiveness of long nanofiller in increasing the normal elastic moduli than the short nanofiller is in concurrence with the similar findings of Liu and Chen (2003a) reported for long and short CNT nanocomposite (only for normal elastic properties). On the contrary, it is interesting to note the slight improvement in the values of shear moduli (except G_{23} of CNT nanocomposite) of nanocomposites when the length of the nanofiller is shortened.

9. Conclusions

In this paper, an initial study is conducted to compare the elastic constants of CNT and graphene reinforced nanocomposites for a given matrix material and volume fraction. Graphene- and CNT-reinforced nanocomposites having different matrix materials are also compared in terms of variations in its stiffness properties. Moreover, effects of volume fraction on elastic stiffness constants of CNT and graphene reinforced nanocomposites are also investigated. Finally, a comparison of elastic properties of nanocomposites embedded with long and short CNT and graphene reinforcements is made.

Based on the results of the present investigation, following important conclusions can be drawn:

- Irrespective of the matrix materials and volume fractions, CNT and graphene reinforced nanocomposites show, respectively, transversely isotropic and orthotropic behaviour with extensional stiffness in the axial direction (i.e., E_1) being almost same for both kinds of reinforcement.
- For all volume fractions and matrix materials, normal modulus, E_2 and shear modulus in plane 1-2, G_{12} are better improved in the case of graphene nanocomposites than CNT nanocomposites; whereas out-of-plane normal modulus E_3 and shear moduli G_{13} and G_{23} in planes 1-3 and 2-3, respectively, are more for CNT nanocomposites.
- Effects of matrix material on normal modulus, E_1 and shear modulus, G_{12} are very significant for graphene nanocomposites which are improved with the increase in E_f/E_m ratio (i.e., when the matrix material becomes less stiff as compared to graphene material), but in the case of CNT nanocomposites, matrix material has substantial effect only on normal modulus, E_1.
- Graphene reinforced nanocomposites shows better in-plane bi-directional stiffening effects than CNT reinforcement which is attributed to the biaxial stiffness properties of a 2-D graphene sheet.

Long nanofillers (graphene as well as CNT) result in increase in the normal elastic moduli of the resulting nanocomposites as compared to the short length reinforcement; on the contrary, the values of shear moduli, except G_{23} of CNT nanocomposite, of nanocomposites are slightly improved in the case of short length nanofillers (i.e., CNT or graphene).

Acknowledgments

The present research work is carried out by utilizing the computation research facilities at the Material Research Centre (MRC), Malaviya National Institute of Technology (MNIT) Jaipur. The authors would like to kindly acknowledge the MRC, MNIT Jaipur.

References

Al-Ostaz, A., Pal, G., Mantena, P.R. and Cheng, A. (2008), "Molecular dynamics simulation of SWCNT – polymer nanocomposite and its constituents", *J. Mater. Sci.*, **43**(1), 164-173.

Arash, B., Park, H.S. and Rabczuk, T. (2015), "Tensile fracture behavior of short carbon nanotube reinforced polymer composites: A coarse-grained model", *Compos. Struct.*, **134**, 981-988.

Arash, B., Park, H.S. and Rabczuk, T. (2016), "Coarse-grained model of the J-integral of carbon nanotube reinforced polymer composites", *Carbon*, **96**, 1084-1092.

Aydogdu, M. (2014), "On the vibration of aligned carbon nanotube reinforced composite beams", *Adv. Nano Res., Int. J.*, **2**(4), 199-210.

Besseghier, A., Heireche, H., Bousahla, A.A., Tounsi, A. and Benzair, A. (2015), "Nonlinear vibration properties of a zigzag single-walled carbon nanotube embedded in a polymer matrix", *Adv. Nano Res., Int. J.*, **3**(1), 29-37.

Bower, C., Rosen, R., Jin, L., Han, J. and Zhou, O. (1999), "Deformation of carbon nanotubes in nanotube–polymer composites", *Appl. Phys. Lett.*, **74**(22), 3317-3319.

Bu, H., Chen, Y., Zou, M., Yi, H., Bi, K. and Ni, Z. (2009), "Atomistic simulations of mechanical properties of graphene nanoribbons", *Phys. Lett. A*, **373**(37), 3359-3362.

Chen, X.L. and Liu, Y.J. (2004), "Square representative volume elements for evaluating the effective material properties of carbon nanotube-based composites", *Comput. Mater. Sci.*, **29**(1), 1-11.

Cho, J. and Sun, C.T. (2007), "A molecular dynamics simulation study of inclusion size effect on polymeric nanocomposites", *Comput. Mater. Sci.*, **41**(4), 54-62.

Coleman, J.N., Khan, U., Blau, W.J. and Gun'ko, Y.K. (2006), "Small but strong: A review of the mechanical properties of carbon nanotube–polymer composites", *Carbon*, **44**(9), 1624-1652.

Geim, A.K. and Novoselov, K.S. (2007), "The rise of graphene", *Nature*, **6**(3), 183-191.

Ghasemi, H., Rafiee, R., Zhuang, X., Muthu, J. and Rabczuk, T. (2014), "Uncertainties propagation in metamodel-based probabilistic optimization of CNT/polymer composite structure using stochastic multi-scale modeling", *Comput. Mater. Sci.*, **85**, 295-305.

Ghasemi, H., Brighenti, R., Zhuang, X., Muthu, J. and Rabczuk, T. (2015), "Optimal fiber content and distribution in fiber-reinforced solids using a reliability and NURBS based sequential optimization approach", *Struct. Multidiscip. Optim.*, **51**(1), 99-112.

Halpin, J.C. (1969), "Effects of environmental factors on composite materials", Technical Report; Air Force Mater. Lab Wright-Patterson AFB OH.

Hyer, M.W. (1998), *Stress Analysis of Fiber-Reinforced Composite Materials*, McGraw-Hill, Boston, MA, USA.

Iijima, S. (1991), "Helical microtubules of graphitic carbon", *Nature*, **354**(6348), 56-58.

Joshi, P. and Upadhyay, S.H. (2014), "Evaluation of elastic properties of multi walled carbon nanotube reinforced composite", *Comput. Mater. Sci.*, **81**, 332-338.

Joshi, U.A., Sharma, S.C. and Harsha, S.P. (2011), "Analysis of elastic properties of carbon nanotube reinforced nanocomposites with pinhole defects", *Comput. Mater. Sci.*, **50**(11), 3245-3256.

Kim, H. and Macosko, C.W. (2009), "Processing-property relationships of polycarbonate/graphene composites", *Polymer*, **50**(15), 3797-3809.

Kondo, D., Sato, S. and Awano, Y. (2008), "Self-organization of novel carbon composite structure: Graphene multi-layers combined perpendicularly with aligned carbon nanotubes", *Appl. Phys. Express.*, **1**(7), 0740031-0740033.

Kuilla, T., Bhadra, S., Yao, D., Kim, N.H., Bose, S. and Lee, J.H. (2010), "Recent advances in graphene based polymer composites", *Prog. Polym. Sci.*, **35**(11), 1350-1375.

Laurent, C., Flahaut, E. and Peigney, A. (2010), "The weight and density of carbon nanotubes versus the number of walls and diameter", *Carbon*, **48**(10), 2994-2996.

Li, C. and Chou, T.-W. (2009), "Failure of carbon nanotube/polymer composites and the effect of nanotube waviness", *Compos. Part A: Appl. Sci. Manuf.*, **40**(10), 1580-1586.

Liu, Y.J. and Chen, X.L. (2003a), "Continuum models of carbon nanotube-based composites using the boundary element method", *Electron. J. Bound. Elem.*, **1**(2), 316-335.

Liu, Y.J. and Chen, X.L. (2003b), "Evaluations of the effective material properties of carbon nanotube-based composites using a nanoscale representative volume element", *Mech. Mater.*, **35**(1-2), 69-81.

Mousavi, A.A., Arash, B., Zhuang, X. and Rabczuk, T. (2016), "A coarse-grained model for the elastic properties of cross linked short carbon nanotube/polymer composites", *Compos. Part B: Eng.*, **95**, 404-411.

Potts, J.R., Dreyer, D.R., Bielawski, C.W. and Ruoff, R.S. (2011), "Graphene-based polymer nanocomposites", *Polymer*, **52**(1), 5-25.

Qian, D., Dickey, E.C., Andrews, R. and Rantell, T. (2000), "Load transfer and deformation mechanisms in carbon nanotube-polystyrene composites", *Appl. Phys. Lett.*, **76**(20), 2868-2870.
Reith, D., Meyer, H. and Müller-Plathe, F. (2001), "Mapping atomistic to coarse-grained polymer models using automatic simplex optimization to fit structural properties", *Macromolecules*, **34**(7), 2335-2345.
Reith, D., Putz, M. and Mller-Plathe, F. (2003), "Deriving effective mesoscale potentials from atomistic simulations", *J. Comput. Chem.*, **24**(13), 1624-1636.
Ru, C.Q. (2001), "Axially compressed buckling of a doublewalled carbon nanotube embedded in an elastic medium", *J. Mech. Phys. Solids*, **49**(6), 1265-1279.
Ruoff, R.S., Qian, D. and Liu, W.K. (2003), "Mechanical properties of carbon nanotubes: theoretical predictions and experimental measurements", *Comptes. Rendus. Phys.*, **4**(9), 993-1008.
Rzepiela, A.J., Louhivuori, M., Peter, C. and Marrink, S.J. (2011), "Hybrid simulations: combining atomistic and coarse-grained force fields using virtual sites", *Phys. Chem. Chem. Phys.*, **13**(22), 10437-10448.
Sakhaee-Pour, A. (2009), "Elastic properties of single-layered graphene sheet", *Solid State Commun.*, **149**(1-2), 91-95.
Salvetat, J.-P., Briggs, G. and Bonard, J.-M. (1999), "Elastic and shear moduli of single-walled carbon nanotube ropes", *Phys. Rev. Lett.*, **82**(5), 944-947.
Sears, A. and Batra, R.C. (2004), "Macroscopic properties of carbon nanotubes from molecular-mechanics simulations", *Phys. Rev. B*, **69**(23), 235406.
Segurado, J., González, C. and LLorca, J. (2003), "A numerical investigation of the effect of particle clustering on the mechanical properties of composites", *Acta Mater.*, **51**(8), 2355-2369.
Semmah, A., Bég, O.A., Mahmoud, S.R., Heireche, H. and Tounsi, A. (2014), "Thermal buckling properties of zigzag single-walled carbon nanotubes using a refined nonlocal model", *Adv. Mater. Res., Int. J.*, **3**(2), 77-89.
Shokrieh, M.M. and Rafiee, R. (2010a), "Prediction of Young's modulus of graphene sheets and carbon nanotubes using nanoscale continuum mechanics approach", *Mater. Des.*, **31**(2), 790-795.
Shokrieh, M.M. and Rafiee, R. (2010b), "On the tensile behavior of an embedded carbon nanotube in polymer matrix with non-bonded interphase region", *Compos. Struct.*, **92**(3), 647-652.
Silani, M., Ziaei-Rad, S., Talebi, H. and Rabczuk, T. (2014), "A semi-concurrent multiscale approach for modeling damage in nanocomposites", *Theor. Appl. Fract. Mech.*, **74**, 30-38.
Sohlberg, K., Sumpter, B.G., Tuzun, R.E. and Noid, D.W. (1998), "Continuum methods of mechanics as a simplified approach to structural engineering of nanostructures", *Nanotechnology*, **9**(1), 30-36.
Stankovich, S., Dikin, D.A., Dommett, G.H.B., Kohlhaas, K.M., Zimney, E.J., Stach, E.A., Piner, R.D., Nguyen, S.T. and Ruoff, R.S. (2006), "Graphene-based composite materials", *Nature*, **442**(7100), 282-286.
Sun, C.T. and Vaidya, R.S. (1996), "Prediction of composite properties from a representative volume element", *Compos. Sci. Technol.*, **56**(2), 171-179.
Talebi, H., Silani, M., Bordas, S.P.A., Kerfriden, P. and Rabczuk, T. (2014), "A computational library for multiscale modeling of material failure", *Comput. Mech.*, **53**(5), 1047-1071.
Tsai, J.-L. and Tu, J.-F. (2010), "Characterizing mechanical properties of graphite using molecular dynamics simulation", *Mater. Des.*, **31**(1), 194-199.
Vu-Bac, N., Rafiee, R., Zhuang, X., Lahmer, T. and Rabczuk, T. (2015a), "Uncertainty quantification for multiscale modeling of polymer nanocomposites with correlated parameters", *Compos. Part B: Eng.*, **68**, 446-464.
Vu-Bac, N., Silani, M., Lahmer, T., Zhuang, X. and Rabczuk, T. (2015b), "A unified framework for stochastic predictions of mechanical properties of polymeric nanocomposites", *Comput. Mater. Sci.*, **96**, 520-535.
Wang, Q., Dai, J., Li, W., Wei, Z. and Jiang, J. (2008), "The effects of CNT alignment on electrical conductivity and mechanical properties of SWNT/epoxy nanocomposites", *Compos. Sci. Technol.*, **68**(7-8), 1644-1648.
Wong, E.W., Sheehan, P.E. and Lieber, C.M. (1997), "Nanobeam mechanics: elasticity, strength, and

toughness of nanorods and nanotubes", *Science*, **277**(5334), 1971-1975.
Xu, Y., Bai, H., Lu, G., Li, C. and Shi, G. (2008), "Flexible graphene films via the filtration of water-soluble noncovalent functionalized graphene sheets", *J. Am. Chem. Soc*., **130**(18), 5856-5857.
Zhang, Y., Zhuang, X., Muthu, J., Mabrouki, T., Fontaine, M., Gong, Y. and Rabczuk, T. (2014), "Load transfer of graphene / carbon nanotube / polyethylene hybrid nanocomposite by molecular dynamics simulation", *Compos. Part B*, **63**, 27-33.
Zhu, Y., Murali, S., Cai, W., Li, X., Suk, J.W., Potts, J.R. and Ruoff, R.S. (2010), "Graphene and graphene oxide: Synthesis, properties, and applications", *Adv. Mater*., **22**(35), 3906-3924.

CC

Nomenclature

a and b	Sides of square RVE
u_{11}, u_{22} and u_{33}	Displacement in *z*, *y* and *x* directions respectively
δ_1, δ_2 and δ_3	Deformation of faces in *x*, *y* and *z* direction, subjected to loading conditions
δ_t, δ_l	Deformation of faces subjected to transverse and longitudinal shear loading conditions respectively
σ_{ij}, ε_{kl} and C_{ijkl}	Stress, strain and stiffness tensor respectively
$\overline{\sigma_{ij}}$ and $\overline{\varepsilon_{kl}}$	Volumetric average of stress and strain of RVE
C^e_{ijkl}	Effective stiffness tensor
ν_{12}, ν_{13} and ν_{23}	Poisson's ratios corresponding to *x*-*y*, *x*-*z* and *y*-*z* planes
E_1, E_2 and E_3	Young's moduli in the *x*, *y* and *z* direction respectively
V_{RVE}	Volume of represented volume element
V_f	Volume fractions for CNT and graphene reinforced RVE
ν_m, ν_{CNT}	Poisson's ratios of matrix and CNT
G_{12}, G_{13} and G_{23}	Shear Modulus corresponding to *x*-*y*, *x*-*z* and *y*-*z* planes
ξ	Reinforcing factor
r_o and r_i	External and internal radius of the CNT
L_1 and L	Length of reinforcement and RVE respectively
w and t	Width and thickness of graphene sheet